Dielectric, electrical properties and thermal sensitivity of a lead free rare earth compound with tungsten bronze-type ceramic thermistor

S. Devi and S. Behera

Department of Physics, School of Applied Sciences, Centurion University of Technology & Management, Bhubaneswar, 752050

E-mail: saubhagyalaxmi.behera@cutm.ac.in

Saparjya S and P. R. Das,

Department of Physics, Veer Surendra Sai University of Technology, Burla-768018

mamisana1410@gmail.com, Ph- +91-9438108634

Abstract- A new tungsten bronze ceramic $Na_2Ba_2Gd_2W_2Ti_4Nb_4O_{30}$was prepared using conventional mixed oxide route.The preliminary structural analysis of the compound using room temperature X-ray diffraction (XRD) indicates the formation of single-phase orthorhombic crystal structure.The temperature and frequency dependent dielectric properties (ε_r and tanδ) of the compound exhibits two phase transitions in it. The low temperature phase transition (at 368K) related to structural type (ferroelectric-ferroelectric) and the high temperature (at 638 K) isrelated to the ferroelectric to paraelectric. Thehysteresis loop (electrical polarization versus field) at room temperature confirms the ferroelectric property of the compound.The electrical properties of the material at a wide range of temperature (25–500 °C) and frequencies (1 kHz – 1 MHz) were investigated usingComplex impedance spectroscopy (CIS). Thetemperature dependent impedance properties were used to obtain the various thermistor parameters and their variation with temperature.

1. INTRODUCTION

Environmentally-friendly lead-free ferroelectric materials with the tungsten bronze (TB) structure compounds have attracted particular attention because of their excellent ferroelectric [1], multiferroic [2], photo luminescent [3], electro-optic [4], piezoelectric [5-7] and pyroelectric [8] properties. The expressions $(A_1)_2(A_2)_4(C)_4(B_1)_2(B_2)_8O_{30}$ describes the tungsten-bronze crystal structure, with A_1 and A_2 sites are filled with by the monovalent alkali metal cations K^+, Na^+, Li^+, the divalent alkaline earth metal ions Sr^{2+}, Ba^{2+}, Ca^{2+}, Pb^{2+} or the trivalent rare-earth metal cations La^{3+}, Nd^{3+}, Eu^{3+}, Gd^{3+}; the B sites are filled by Nb^{5+}, Ta^{5+}, Zr^{4+}, Ti^{4+}, Sb^{5+}; and the C sites by Li^+, Be^{2+}, Mg^{2+}. Generally, in the several chemical bonds of the tungsten-bronze structure, ferroelectricity arises due to interaction between the B atom and its surrounding oxygen framework in the BO_6 polar unit [9,10]. The C sites being the smallest and are generally empty. When all the six A site cations are occupied in the structure $(A_1)_2(A_2)_4(C)_4(B_1)_2(B_2)_8O_{30}$, it represents a 'filled' TB structure; otherwise it is referred to an 'unfilled' TB [11–12]. It has been found that different ionic size substitutions at the above-mentioned sites (A and B) can tailor their

physical properties for device applications. Recent studies reveal that a lot of work has been carried out on lead based tungsten-bronze ferroelectricniobateceramics with rare earth ions for their exciting electrical properties [13-15]. So we are searching for a lead-free ferroelectric, as the ferroelectrics containing lead is hazardous to human-beings and environment [16]. Again, the niobates consist of corner-sharing NbO6 octahedra which arrangement gives three kinds of interstitial sites which can be occupied by Ba, Sr, Ca, Na, or other elements with similar size. So the dielectric and ferroelectric properties and compositions of these niobate-based -ceramics can be adjusted[17,18]. Hence we have synthesized a new complex environment-friendly lead-free TB-structured niobate, $Na_2Ba_2Gd_2W_2Ti_4Nb_4O_{30}$ (NBGWTN), and studied its structural and electrical properties.

2. EXPERIMENTAL PROCEDURE:

The Polycrystalline sample of $Na_2Ba_2Gd_2W_2Ti_4Nb_4O_{30}$ (abbreviated as NBGWTN) was prepared by high temperature solid state reaction technique using high purity ingredients Na_2CO_3(99%, Merck), $BaCO_3$(99%, Merck), Gd_2O_3, WO_3(99.9%, M/s. LobaChemie Pvt. Ltd., India), TiO_2 (99%, Merck), and Nb_2O_5(99.9%,Puriss AR). These ingredients are taken in suitable stoichiometric ratio and were thoroughly mixed and ground in dry and wet (methanol) medium for 1 h each in an agate mortar. Calcination was carried out at 1150 ^{0}C for 4 h for the samples by using an alumina crucible. The process of grinding and calcinations were repeated to ensure the completion of reaction. The quality and formation of the compound were checked by an X-ray diffraction (XRD) technique using an x-ray powder diffractometer (RigakuUltima IV, Japan)with CuK_α radiation ($\lambda = 1.5405$ Å) over a wide range of Bragg angles 2θ ($20° \leq 2\theta \leq 80°$).The powder was then pressed into pellets (10 mm diameter and thickness 1 mm to 2 mm) under the uniaxial pressure of 3.5 ton by using a hydraulic press. Polyvinyl alcohol (PVA) was used as binder during preparation of pellets. The pellets were then sintered at 1200 ^{o}C for 4 h in a covered alumina crucible in air atmosphere. The binder was burnt out during the sintering process. The sintered pellets were then polished with fine emery paper in order to make both faces flat and parallel. After that the pellets were electroded with high quality silver paste and then dried at 150 ^{o}C for 1 h in order to remove moisture before taking any electrical measurements. The dielectric, impedance and modulus parameters of a silver-electroded pellet were measured as a function of frequency (1 kHz to 1 MHz) by using a computer-controlled HIOKI 3532 LCR Hitester over a wide range of temperature.

3. RESULTS AND DISCUSSION

3.1 Structural Andmicrostructural Studies

The X-ray diffraction (XRD) pattern of NBGWTN at room temperature of the calcined powder sample is shown in Figure 1(a). All the peaks were smoothened. The sharp and single diffraction peaks are different from that of the precursors thus indicating that single-phase new compound isformed and moreover suggestenhanced crystallization and better homogeneity of the resultant material.All the peaks of the XRD patterns wereindexed by taking 2θ and intensity value of each peak using the standard computer software 'POWD'. The best agreement between the observed and the calculated interplanarspacings (d) and Bragg angles was found for the orthorhombic crystal

structure. The least-squares refined unit cell parameters are: a = 23.9300 Å, b = 16.6976 Å, c = 3.5100 Å and volume V = 1403.50 $Å^3$ with standard deviation of 0.0036. The refined lattice parameters of the material are found to be consistent with the reported compounds having similar structure. It was not possible to find out the space group distinctivelywith the limited x-ray powder diffraction data [19].

Further, the crystallite or particle size (P) of the compound was calculated using the broadening of some widely spread (over Bragg angles) strong and medium reflections in the Scherrer's equation: $P_{hkl} = \frac{K\lambda}{\beta_{1/2} Cos\theta_{hkl}}$ [20],where k (constant) = 0.89, λ=1.5405^{0}A and $\beta_{1/2}$= full width at half maximum (in radians). The average value of P_{hkl} is found to be 19.39nm.

The SEM micrograph ofNBGWTN is shown in Fig. 1 (inset).The nature (size, shape and distribution of grains) of the microstructures of the sample suggests that the grain growth has more or less completed during sintering, and hence no secondary phase was observed. Because of some voids of irregular shape, size and dimension very high density sample could not be obtained. In addition to the above, some small size grains were found to be homogenously distributed throughout the surface of the sample. The grain size (from the micrograph) is found to be in the range of 2-8 μm.

3.2 Dielectric Study

Fig 2 (a) & (b) show the temperature variation of relative dielectric constant (ε_r) and tangent loss (tanδ) of the compound at some selected frequency (10kHz, 100kHz and 1MHz). Two dielectric peaks (at 368 K and 638 K) were observed for all the three frequencies. The dielectric constant increases gradually with increase of temperature and attains a maximum value (peak) at 368 K and then decreases. Further, ε_r increases with rising of temperature and attains another peak at 638 K. The rapid increaseofε_r beyond second anomaly is again due to space charge polarization which is dueto mobility of charge carriers and imperfections in the material. Earlier such two phase transitions areobserved in some orthorhombic tungsten bronze ferroelectrics [21–22].According to the observations found in literature, the high temperature anomaly (638 K) may be a ferroelectric—paraelectric transition (Tc), while the lower one (368 K) is assumed to structural type (ferroelectric—ferroelectric) transition. This conclusion demands suitable experiment for confirmation. The ferroelectric to paraelectric transition of the material was confirmed later by polarization study. The frequency independent transition temperatures (no dielectric dispersion), of the compound suggests that it is not anrelaxor. The values of ε_{max} (dielectric constant at Tc_1) at 1, 10, and 50 kHz are found to be 680, 391, 310, and those of at Tc_2 are 2830, 647, 376 respectively which are much higher than that of reported similar lead based compound, $Li_2Pb_2Gd_2W_2Ti_4Nb_4O_{30}$ [22]. The variation of tanδ with temperature follows the similar trend as of ε_r. The values of $\tan\delta_{max1}$ (tangent loss at Tc_1) at same frequency are found to be 8.74, 1.73, 0.57 and those of at Tc_2 are 4.74, 2.68, 1.149 respectively. Further the maximum dielectric constant and dielectric loss at the second transition decreases with increasing frequency which isa characteristic of normal ferroelectric oxide materials. This is due tothe absence of dipolar and ionic polarizations in the material at higher frequency.

Fig. 3 shows the variation of dielectric constant with frequency at different temperatureof the sample. It is observed thatε_r, decreases strongly in the low-frequency region whereas quite slowly in the high-frequency region. This type of dielectric behavior in the sample can be explained by the Maxwell–Wagner and Koop's phenomenological models [23]. According to this model, dielectric medium consists highly conducting grains and poorly conducting grain boundaries. The grains are more effective at higher frequencies while at lower frequencies the grain boundaries are more effective. The dielectric constant (ε_r) decreases with rising frequency which is may be due to the fact that the electron hopping between Ti^{4+}– Ti^{3+} at octahedral sites cannot follow the alteration of ac electric field at higher frequencies. Therefore, electrons have to passthrough the well conducting grains and the poorly conducting grain boundaries. As the grain boundaries have large resistance, the electrons pileup there and produce large space charge polarization. Therefore, $\varepsilon_r$is more in the low-frequency range. On further increasing at lower frequencies at lower frequencies frequency, the electrons change their direction of motion rapidly, which hinders the movement of electrons inside the dielectric materials and thus accumulation of charges at the grain boundaries decreases and hence decreases the ε_r.

3.2 Impedancespectroscopy Study

ComplexImpedance Spectroscopy (CIS) is a powerfultechniquefor electrical characterization of materials over a wide range of temperature and frequency. By this method one can be able to differentiateamong(i) bulk, (ii) grain boundary, (iii) electrode polarization effect of the material. An ac signal is applied through the pellet sample, and its output response is measured. The data for impedance measurements of the materials has both real (resistive) and imaginary (reactive) components. For this purpose certain basic equations of impedance and electrical modulus are used in this method:

Complex impedance, $Z(\omega) = Z' - jZ'' = R_s - \frac{j}{\omega C_s}$;

Complex electrical modulus, $M(\omega) = \frac{1}{\varepsilon\omega} = M' + jM'' = j\,\omega C_0 Z$;

Complex admittance, $Y^* = Y' + jY'' = j\omega C_0 \varepsilon = (R_p)^{-1} + j\omega C_p$

Complex permittivity, $\varepsilon^* = \varepsilon' - j\varepsilon''$, where $\omega = 2\pi f$ is the angular frequency, C_0 is the geometrical capacitance, and the subscripts "p" and "s" indicate parallel and series components, respectively. By using above equations we will get resultant impedance and modulus formalism to compute and study the detail electrical properties of the materials.

Figure 4 (a) shows the variation of Z' with frequency at different temperatures is shown in figure4(a). From the graph, the magnitude of Z' decreases with increase in both frequency as well as temperature, indicating an increase in AC conductivity.The Z' values for alltemperatures merge at high frequency which may be due to the release of space charge, as a result ofreduction in barrier properties of the material with rise in temperature [24]. Again at low frequency region Z' decreases with rise in temperature indicating negative temperature coefficient of resistance

(NTCR)- type behavior of the material similar to that of semiconductors. Figure4 (b) shows the variation of Z"with frequency at different temperatures. TheZ" values for all the temperatureattains maximumat a particular frequency (known as relaxation frequency,f_r) which explains the presence of relaxation in the sample[25].Inverse of f_r is known as relaxation time of the sample. The peak ($Z"_{max}$)shifts toward higher frequency side with rise of temperature suggesting that the relaxation time decreases with rise in temperature i.e. temperature dependent relaxation phenomena in the material.Generally,immobile charges at low temperatures and defects/vacancies at higher temperatures are responsible forrelaxation process in dielectric material [26].The asymmetric broadening of the peaks suggests the spreading of relaxation with temperature and consiststwo equilibrium positions. The peak heights are proportional to bulk resistance (R_b), and can be explained by the equation$Z''[=R_b\{\frac{\omega\tau}{1+\omega^2\tau^2}\}]$ in Z" versus frequency plot. Due to the above cause the the peak heights decreases with temperature.

Fig. 5.shows the variation of ln τ (relaxation time) with inverse of absolute temperature (10^3/T). With increase in temperature the value of τ decreases. The plot follows the Arrhenius relation : $\tau = \tau_0 \exp(-Ea/kT)$. Using the above relation, the activation energy (Ea) was found to be 0.71 eV.

The Nyquist plot or Cole–Cole plot is also another important technique to study the relaxation and conduction processes.It calculates different parameters associated with grain and grain boundary effects.

The temperature dependent complex impedance spectra (Nyquist plot) over a wide frequency range (1 kHz-1 MHz) of the sample is shown in Fig 6. The impendence appears as semicircular arcs whose pattern changes with rise in temperature.The plot indicates that the area of the semicircle decreases with increasing temperature , highlightingdecrease in resistivity with increasing temperature At low temperature (up to 200^0C), complex impedance plots have single semicircular arc whereas, at higher temperatures (above 200^0C), two semicircular arcs (with center just below the real axis) are observed. It is found that most acceptable approach to interpret the depression of semicircles is statistical distribution of relaxation time [27]. The nature of plots suggests that the electrical response is composed of at least two semicircles, first due to bulk (grain) property of material whereas the second one (at high temperature) is due to presence of grain boundary [28]. Fig. 5 compares the complex impedance plots with fitted data using commercially available software ZSIMP WIN version 2. The analysis of the curves shows that the semicircle exhibits some depression instead of a semicircle centered on the abscissa axis confirming spread of relaxation with non-Debye type. In an ideal case (Debye-like response) an equivalent circuit has parallel combination of CQR and CR where Q is known as constant phase element (CPE), R is the resistance and C is the capacitance. The admittance of Y of CPE is defined as $Y^*(CPE) = A_0 (j\omega)^n = A\omega^n + jB\omega^n$, where $A = A_0 \cos(n\pi/2)$ and $B = A_0 \sin(n\pi/2)$. A0 and n are frequency independent but temperature dependent parameters, A_0 determines the magnitude of the dispersion and it varies between zero and one ($0 \leq n \leq 1$). The CPE describes an ideal capacitor for n = 1 and an ideal resistor for n = 0 [29].From this fitted curves, the value of bulk resistance (R_b) at different temperatures was calculatedand plotted in fig 7. It clearly shows that the parameters R_b decreases with rise in temperature once again suggestingthe NTCR behavior of the material [28].

3.3 Thermistor Constant beta (β) or Sensitivity

The high value of reisistance obtained in the material makesit more suitable for thermistor application.

The variation of resistane with temeperature follows an empirical relation given by

$$R = R_0 \exp\left(\frac{-E_a}{K_B T}\right) \text{or} R = R_0 \exp \beta\left(\frac{1}{T} - \frac{1}{T_0}\right) \quad (1)$$

Where R is the resistance of thermistor at the temperature T (K), R_0 is the resistance at given temperature T_0(K) and β is the material specific constant. It is observed that the resistance varies with temperature indicating that the material can be used as NTC thermistor [30]. The NTC thermistor parameter (β) can be calculated by using the following relation

$$\beta = \frac{ln\left(\frac{R_{T1}}{R_{T2}}\right)}{\left(\frac{1}{T_1} - \frac{1}{T_2}\right)}$$

Where R_{T1}= Resistance at Temperature 1,R_{T2}= Resistance at Temperature 2

T_1 =Temperature1 (K), T_2= Temperature 2 in (K)

The β value describes the thermistor specification and components [31]. The change of β value with temperature is revealed in Fig. 8 and found that β increases with increase in temperature for the material. It is found in literature that for good thermal sensing applications, the value of β must lies between 4000K-15000K [32]. In our study, the value of β is obtained in the range of 2000K-8000K, which confirms that the material have high temperature stability property and very much appropriate for high temperature electronics applications.

The α value (temperature coefficient) for a thermistor can be calculated using Steinhart-Hart coefficient is given below.

$$\alpha = \frac{-\beta}{T^2}$$

The αvalues explain the material characteristics which are defined as the change of percentage in resistance per unit degree or temperature coefficient. The variation the α value with temperature for the compound is shown in Fig 9 and a nonlinear behavior was observed.The thermistor sensitivity described by the activation energy which is calculated by the equation Ea=kB×β where Ea is the activation energy, kB is the Boltzmann constant and β is the thermistor constant. The activation energy variation with temperature is shown in Fig 10 and found that activation energy increases with temperature. The plot shows the transition from lower value to higher value, which is significant for industrial purpose.

3.4 Polarization Study

The ferroelectric nature of the materials is usually confirmed by the hysteresis loop. In general, a hysteresis loop indicates the occurrence of energy loss in a material with the amount being proportional to the area of the loop. The

electric field-induced polarization (P-E) hysteresis loop for NBGWTN at room temperature is shown in Figure 11. The figure reveals that the remanent polarization of NBGWTN is 0.573 $\mu C/cm^2$formaximum applied electric field E_{max}= 1.251 kV/cm. The remanent polarization obtained for the material is small but P~E curve confirms that the sample is ferroelectric in nature [33].

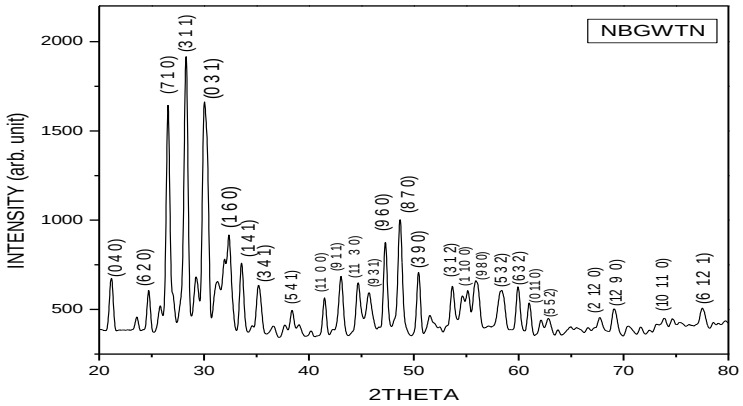

Fig. 1 (a)

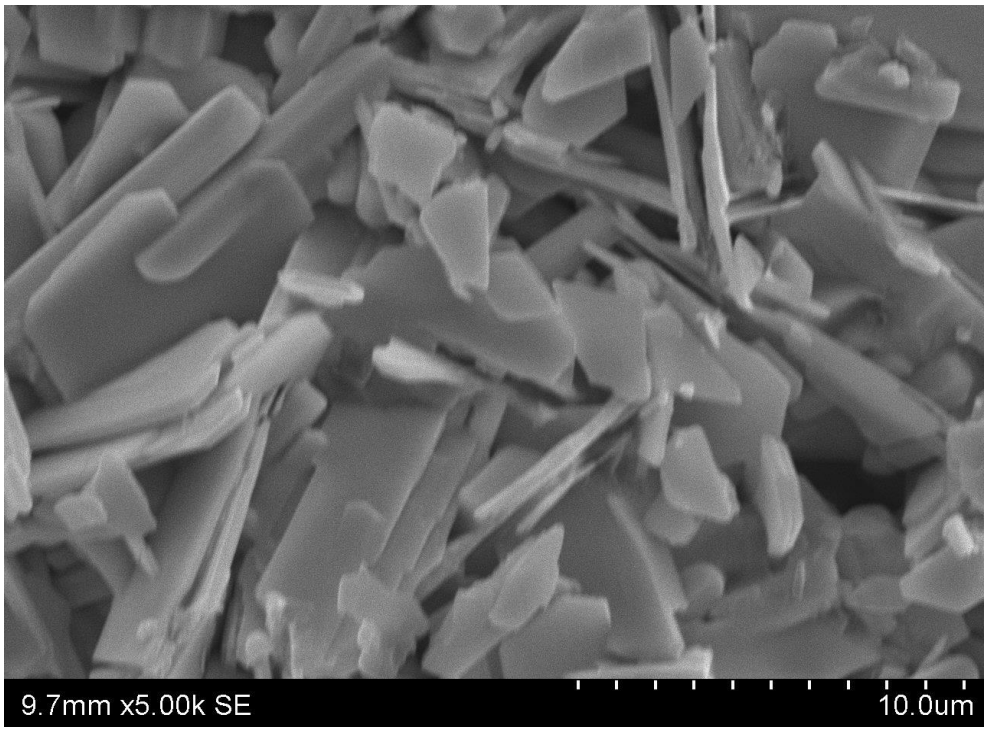

Fig. 1(b)

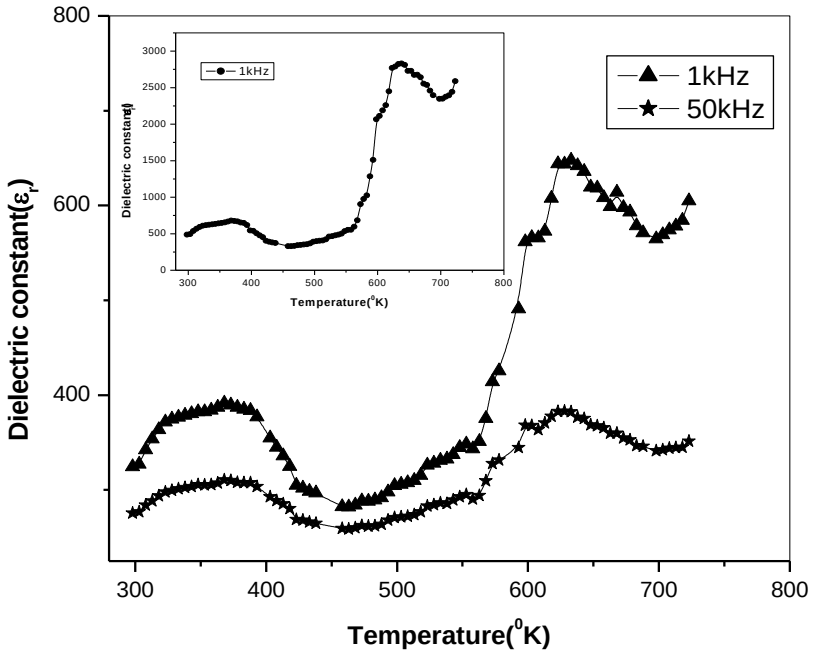
Dielectric constant(ε_r)
Temperature(⁰K)
1kHz
50kHz
Dielectric constant(ε_r)
Temperature(⁰K)
1kHz

Fig. 2 (a)

Fig. 2 (b)

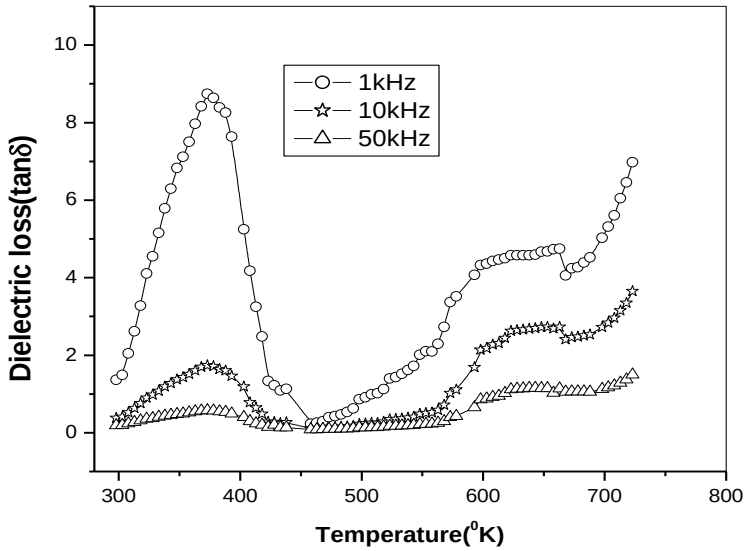
Dielectric loss(tanδ)
Temperature(⁰K)
1kHz
10kHz
50kHz

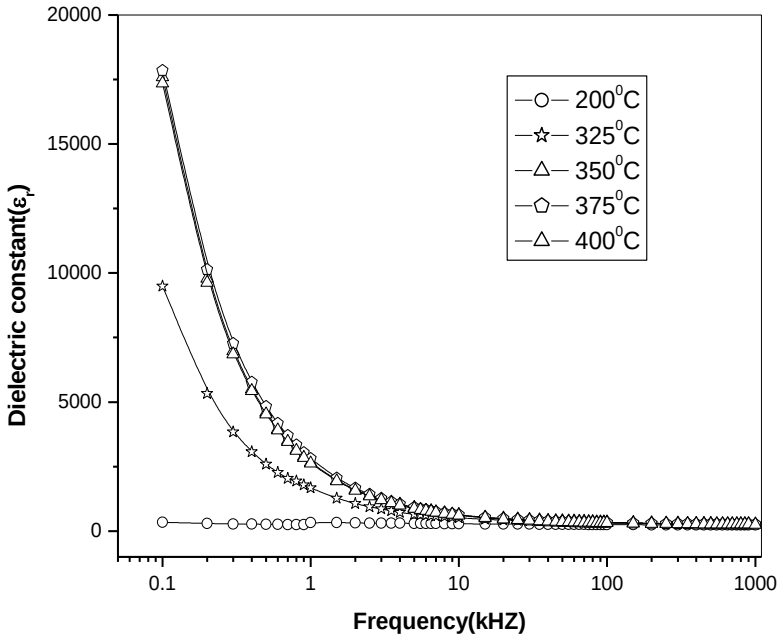
20000
15000
10000
5000
0
Dielectric constant(ε_r)
0.1
1
10
100
1000
Frequency(kHZ)
200°C
325°C
350°C
375°C
400°C

Fig.3

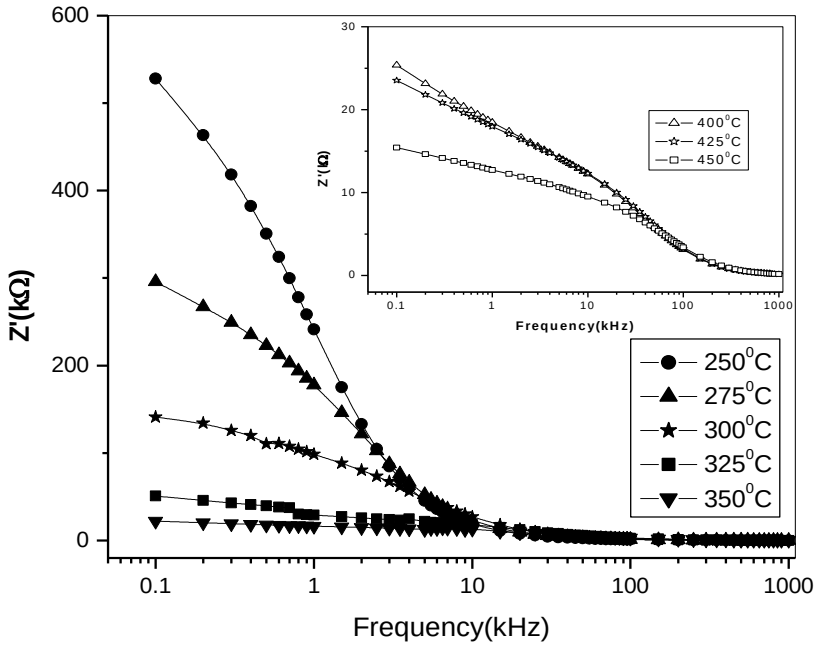
600
400
200
0
Z'(kΩ)
0.1
1
10
100
1000
Frequency(kHz)
250°C
275°C
300°C
325°C
350°C
30
20
10
0
Z'(Ω)
400°C
425°C
450°C
Frequency(kHz)

Fig.4 (a)

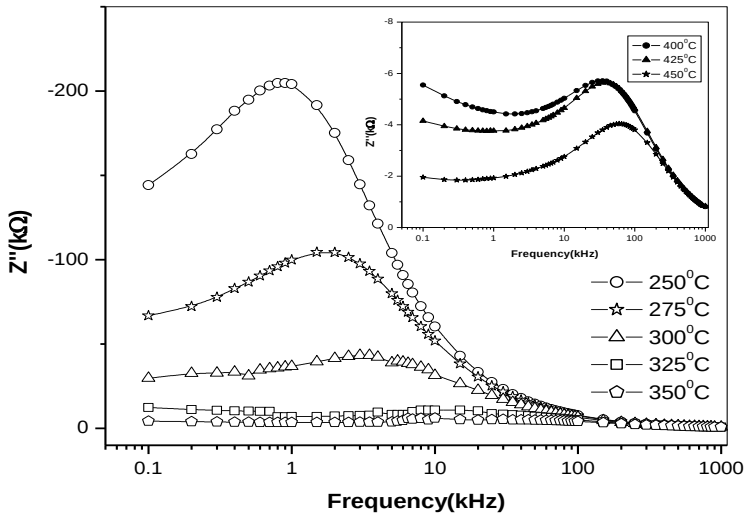
Z''(kΩ)
Frequency(kHz)
250°C
275°C
300°C
325°C
350°C
400°C
425°C
450°C

Fig.4(b)

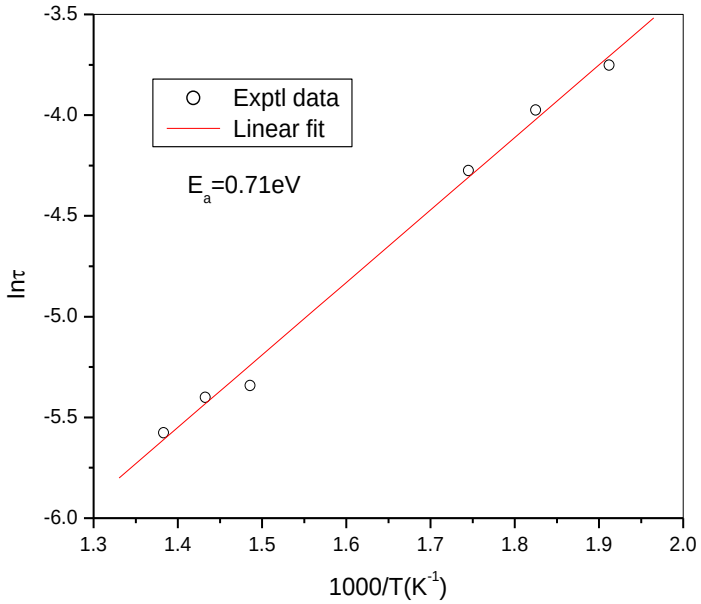
Exptl data
Linear fit
E_a=0.71eV
lnτ
1000/T(K^-1)

Fig.5

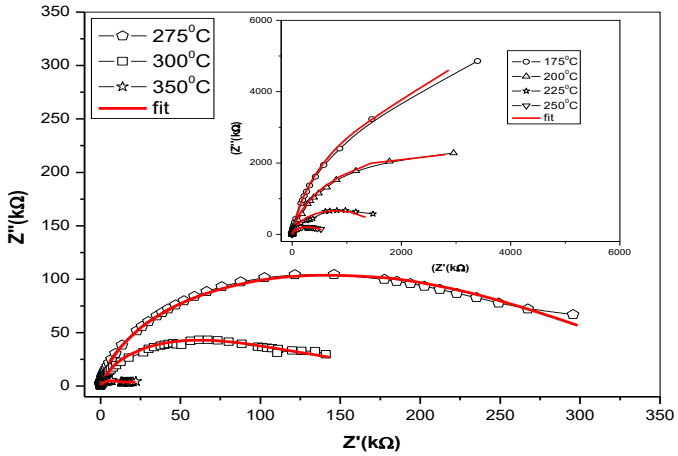

Fig.6

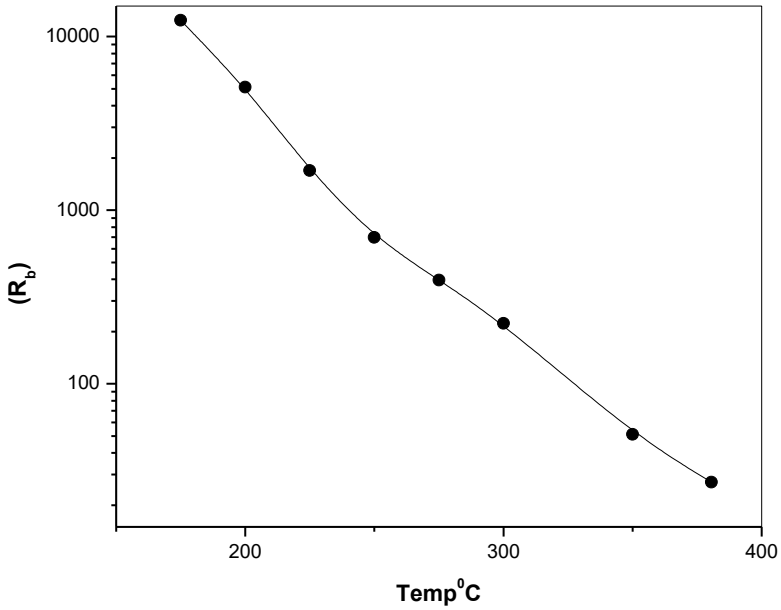

Fig. 7

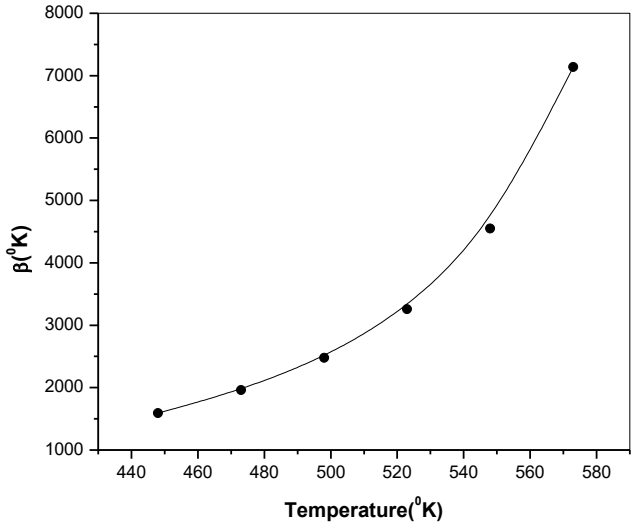
8000
7000
6000
5000
4000
3000
2000
1000
β(⁰K)
440
460
480
500
520
540
560
580
Temperature(⁰K)

Fig. 8

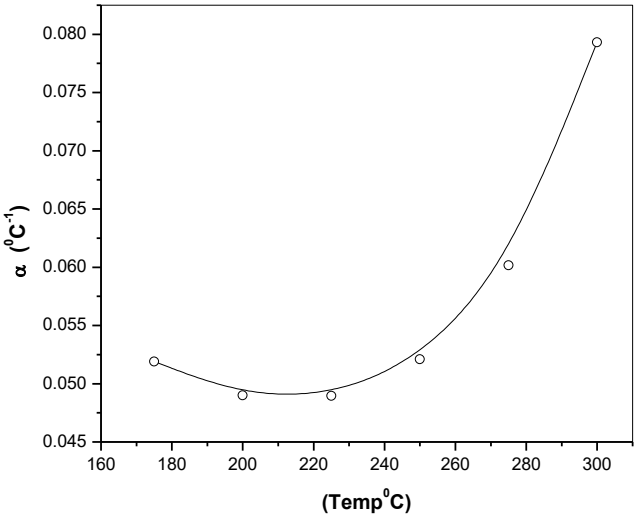
0.080
0.075
0.070
0.065
0.060
0.055
0.050
0.045
α (⁰C⁻¹)
160
180
200
220
240
260
280
300
(Temp⁰C)

Fig.9

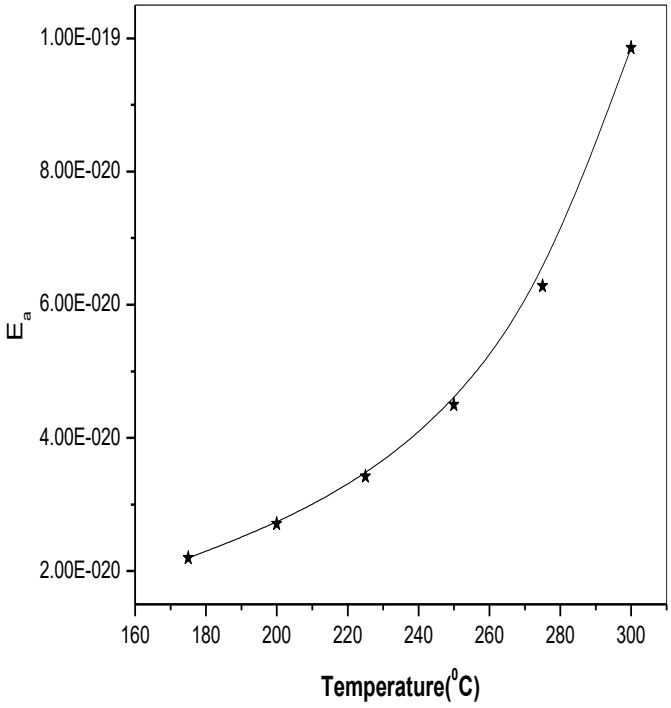
1.00E-019
8.00E-020
6.00E-020
4.00E-020
2.00E-020
E_a
160
180
200
220
240
260
280
300
Temperature(^{0}C)

Fig.10

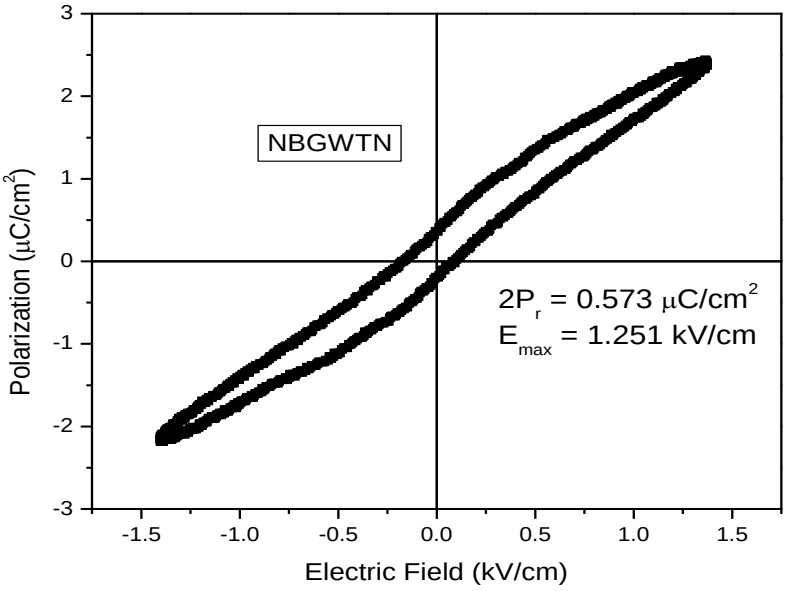
NBGWTN
$2P_r$ = 0.573 μC/cm^2
E_{max} = 1.251 kV/cm
Polarization (μC/cm^2)
Electric Field (kV/cm)
3
2
1
0
-1
-2
-3
-1.5
-1.0
-0.5
0.0
0.5
1.0
1.5

Fig.11

Figure caption

Figure 1: (a) &(b)(XRD & SEM) pattern ofNBGWTN at room temperature.

Figure 2: Temperature dependence of (a) ϵ_r and (b)tanδ ofNBGWTN at different frequencies.

Figure 3: Variation of ϵ_r with frequency of NBGWTN at different temperature.

Figure 4: (a) Variation of Z' with log of frequency of NBGWTN at different temperatures.

(b)Variation of Z'' with log of frequency of NBGWTNat different temperatures.

Figure 5:Variation of relaxation time (τ) as a function of reciprocal of absolute temperature of NBGWTN.

Figure 6:Variation of Z'' with Z' of NBGWTNat different temperatures (Nyquist Plot).

Figure 7: Variation of bulk resistance with temperature of NBGWTN.

Figure 8: Temperature Dependence of β constant of NBGWTN ceramic.

Figure 9: Temperature dependence of α ofNBGWTN ceramic .

Figure 10: Variation of Activation energy with temperature of NBGWTN ceramic.

Figure 11: Hysteresis loop of NBGWTN ceramic.

4. CONCLUSION

The lead free Polycrystalline material of a new ferroelectric compound, $Na_2Ba_2Gd_2W_2Ti_4Nb_4O_{30}$, was prepared by a high-temperature mixed oxide technique. X-ray analysis reveals the orthorhombic crystal structure of the compound at room temperature. The surface morphology of the compound, studied by SEM, gives the grain size in the range of 2-8 μm. Two dielectric anomalies at 368K and 638K may be associated with structural and ferroelectric-paraelectrictransition in this material. Impedance spectroscopy study of the compound shows that the material has (i) conduction due to bulk material up to temperature 200^0C, (ii) NTCR-type behavior and (iii) temperature dependent relaxation phenomena. Various thermistor parameterswere obtained from the temperature dependent impedance study and premier thermistor parameter was obtained which makes the material suitable for thermistor based sensor application.

REFERENCES

[1]. M. Bouziane, M. Taibi, A. Boukhari, "Synthesis and ferroelectric properties of rare earth compounds with tungsten bronze-type structure", *Materials Chemistry and Physics*, 129, (2011), 673– 677.

[2]. E. Castel, P. Veber, M. Albino, M. Velázquez, S. Pechev, D. Denux, J.P. Chaminade, M. Maglione, M. Josse, "Crystal growth and characterization of tetragonal tungsten bronze FerroNiobates $Ba_2LnFeNb_4O_{15}$",Journal of Crystal Growth,340, (2012) 156–165.

[3]. T. Wei, Y.Q. Wang, C.Z. Zhao, L.Q. Zhan, "Photoluminescence and electrical characterization of unfilled tetragonal tungsten bronze $Ba_4La_{1-x}Eu_xTiNb_9O_{30}$", *Materials Research Bulletin*,60, (2014). 111–117,

[4]. T. Wei, Y.Q.Wang, Q.J.Zhou, Z.P.Li, L.Q.Zhan, Q.Jin, "Bright reddish-orange emission and enhanced electrical properties of Sm-doped unfilled tetragonal tungsten bronze Ba4LaTiNb9O30", *Ceramics International*, 40, (2014),16647–16651.

[5]. Shujun Zhang, FapengYu,"Piezoelectric Materials for High Temperature Sensors",J.Am.Ceram.Soc.,94, (2011),3153–3170.

[6]. Jing-jing Yuan, Xiao-ming Chen, Jian-ping Zhou, Peng Liu, "Microstructure, dielectric and piezoelectric properties of $(Pb_{1-x}Sr_x)Nb_{1.96}Ti_{0.05}O_6$ ceramics", Solid State Sciences, 35, (2014), 74–80.

[7]. Y.B. Yao, C.L. Mak, "Effects of Ca-dopant on the pyroelectric, piezoelectric and dielectric properties of (Sr0.6Ba0.4)4Na2Nb10O30 ceramics", Journal of Alloys and Compounds, 544, (2012) 87–93.

[8]. R. Padhee,P. R. Das,B.N. Parida,S. Behera,R.N.P. Choudhary, "Dielectric and electrical properties of a tungsten bronze tantalate ceramic", Current Applied Physics,13, (2013),1014–1020.

[9]. R.J. Xie, Y. Akimune, Lead-free piezoelectric ceramics in the $(1-x)Sr_2NaNb_5O_{15}$-$xCa_2NaNb_5O_{15}$ ($0.05 \leq x \leq 0.35$) system, J. Mater. Chem. 12 (2002) 3156–3161.

[10]. L.L. Wei, Z.P. Yang, Y.F. Chang, R. Gu, Effect of seeding $Sr_2KNb_5O_{15}$ on the phase formation and microstructural development in reactive sintering of $Sr_2NaNb_5O_{15}$ ceramics, J. Am. Ceram. Soc. 91 (2008) 1077–1082.

[11]. K. Lin, Y.C. Rong, H. Wu, Q.Z. Huang, L. You, Y. Ren, L.L. Fan, J. Chen, X.R. Xing, Ordered structure and thermal expansion in tungsten bronze $Pb_2K_{0.5}Li_{0.5}Nb_5O_{15}$,Inorg. Chem. 53 (2014) 9174–9180.

[12]. W.L. Gao, H.J. Zhang, S.Q. Xia, B.B. Huang, D. Liu, J.Y. Wang, M.H. Jiang,L.M. Zheng, J.F. Wang, C.J. Lu, Effect of doping with Nd^{3+} ions on the structural and ferroelectric properties of $Ca_{0.28}Ba_{0.72}Nb_2O_6$ single crystal, Mater. Res. Bull. 45(2010) 1209–1212.

[13]. B.N. Parida, P.R. Das, R. Padhee, R.N.P. Choudhary, Phase transition and conduction mechanism of rare earth based tungsten-bronze compounds, J. Alloys Comp. 540 (2012) 267.

[14]. P. R. Das, L. Biswal, B.N. Parida, and B. Behera, Diffuse Ferroelectric Phase Transition in$Na_2Pb_2Pr_2W_2Ti_4Nb_4O_{30}$ Ceramic, Int. J. Mat. Sci., 5, (2010), 759—767.

[15]. B. N Parida, P.R. Das, R. Padhee and R N P Choudhary, Synthesis and characterization of a new ferroelectric oxide, Bull. Mater. Sci., (36), (2013), 883–892.

[16]. M. Maeder, D. Damjanovic, N. Setter, Lead free piezoelectric materials, J.Electroceram. 13 (2004) 385–392.

[17]. P. Jamieson, S. Abrahams, J. Bernstein, Ferroelectric tungsten bronze-typecrystal structures I. barium strontium niobate, J. Chem. Phys. 48 (1968), 5048–5057.

[18]. G. Beall, L. Pinckney, Nanophase glass–ceramics, J. Am. Ceram. Soc. 82 (1999)5–16.

[19]. R. Padhee, P.R. Das, B.N. Parida, and R.N.P. Choudhary, "Electrical and Pyroelectric properties of $K_2Pb_2Gd_2W_2Ti_4Nb_4O_{30}$ Ferroelectrics", *Journal of Electronic materials*, Vol. 42(3), (2013).

[20]. B. D. Cullity, Elements of X-ray Diffraction, Addison Wesley, (1978).

[21]. L.Biswal, P.R.Das, B.Behera, R.N.P.Choudhury, "Structural, dielectric and conductivity studies of $Na_2Pb_2La_2W_2Ti_4Nb_4O_{30}$ ferroelectric ceramic",*J.Electroceram.*29 (2012)204–210.

[22]. B. N. Parida P.R. Das, R. Padhee, R.N.P. Choudhary, Synthesis and chracterization of a tungsten bronze ferroeletcric oxide Adv. Mater. Lett. 3 (2012),231–238

[23]. C.G. Koops, Phys. Rev.''On the Dispersion of Resistivity and Dielectric Constant of some Semiconductors at Audiofrequencies" 83 (1951) 121–124.

[24]. P.Ganguly, A.K.Jha, K.L.Deori "Complex impedance studies of tungsten–bronze structured Ba5SmTi3Nb7O30 ferroelectric ceramics", Solid State Comm. 146 (2008) 472–477

[25]. B.N. Parida, P.R. Das, R. Padhee, R.N.P. Choudhary, A new ferroelectric oxide $Li_2Pb_2Pr_2W_2Ti_4Nb_4O_{30}$: Synthesisand characterization, J. Phys. Chem. Solids, 73,(2012) 713

[26]. A.K. Jonscher, The 'universal' dielectric response. Nature. 267 (1977) 673-679.

[27]. M. A. L Nobre, S. Lanfredi, Ferroelectric state analysis in grain boundary of Na0.85Li0.15NbO3 ceramic, J. Appl. Phys. 93 (2003) 5557.

[28]. P.S. Das, P.K. Chakraborty, B. Behera, R.N.P. Choudhary, Electrical properties of$Li_2BiV_5O_{15}$ ceramics, Phys. B 395 (2007) 98-103

[29]. R. Ranjan, R. Kumar, N. Kumar, B. Behera, R.N.P. Choudhury, Impedance and electric modulus analysis of Sm-modified Pb(Zr0.55Ti0.45)1_x/4O3 ceramics,J. Alloys Compd. 509 (2011) 6388-6394.

[30]. K. Park, J.K. Lee, J.G. Kim and S. Nahm, "Improvement in the electrical stability of Mn– Ni–Co–O NTC thermistors by substituting Cr2O3 for Co3O4," Journal of Alloys and Compounds, 437, (2007) 211-214.

[31]. Xinyu Liu, Ying Luo and Xvqiong Li, "Electrical properties of BaTiO3-based NTC ceramics doped by BaBiO3 and Y2O3," Journal of Alloys and Compounds, 459, (2008) 45-50

[32]. W. Luo, H. M. Yao, P. H. Yang, C. S Chen,Negative Temperature Coefficient Material with Low Thermal Constant and High Resistivity for Low-Temperature Thermistor Applications, J Am Ceram Soc, 92 (2009) 2682–2686.

[33]. S.K. Satpathy, N.K. Mohanty, A.K. Behera, S. Sen, B. Behera, & P. Nayak, "Dielectric and Electrical properties of $BiFeO_3$-$PbZrO_3$ composites", Journal of Electronic Materials, 44, (2015), 129.